

## A Two-dimensional Numerical Study of Combustion in Porous Media

### M. BIDI

Faculty of Mechanical Engineering, Amirkabir University of Technology, Department of Mechanical Engineering, Amirkabir University of Technology, 424 Hafez Ave. P.O. Box 15875-4413, Tehran, Iran  
m.bidi@aut.ac.ir

### M. SAFFAR AVVAL

Faculty of Mechanical Engineering, Amirkabir University of Technology, Department of Mechanical Engineering, Amirkabir University of Technology, 424 Hafez Ave. P.O. Box 15875-4413, Tehran, Iran  
mavval@aut.ac.ir

### M. HEYRANI NOBARI

Faculty of Mechanical Engineering, Amirkabir University of Technology, Department of Mechanical Engineering, Amirkabir University of Technology, 424 Hafez Ave. P.O. Box 15875-4413, Tehran, Iran  
mrnobari@aut.ac.ir

**Abstract.** Combustion in Porous Media has interesting advantages compared with free flame combustion due to higher burning rates, increased power dynamic range, extension of the lean flammability limits, and low emissions of pollutants. A numerical code is developed in order to evaluate the effects of different parameters of combustion in porous media. The Navier-Stokes, the solid and gas energy and the chemical species transport equations are solved using a multi-step reduced kinetic mechanism. The discrete ordinates method is used to solve the radiative transfer equation and a finite volume method based on SIMPLE method is applied to discretize the conservation equations. The different burner regions consisting of a preheat zone (low porosity matrix), a combustion zone (high porosity matrix) and a heat exchanger zone are studied in this article and the temperature field and species mass fractions obtained numerically are compared with available experimental data. It is found that using of multi-step chemistry leads to more accurate results for temperature field and species mass fractions. Also at high convective coefficients, the local thermal equilibrium assumption is valid for the gas and the solid phase temperatures.

**Keywords.** Combustion, Porous Media, multi-step mechanism, radiation, finite volume

### 1. Introduction

Combustion in porous media differs significantly from free flames due to two main factors including the high surface area of the porous media resulting in efficient heat transfer between the gas and the solids, and well mixing of fuel and oxidant in porous media increasing effective diffusion and heat transfer in the gas phase. It is an internally self-organized process of heat recuperation.

In the upstream, heat is transferred from solid matrix to inlet fuel-air mixture (preheat effect) and in the downstream, heat of combustion is transferred from hot gas products to solid matrix which in turn radiate to its surrounding. These heat transfer mechanisms lead to increase of temperature up to the adiabatic temperature (Babkin, 1993). Superadiabatic combustion significantly extends the lean flammability limit to equivalence ratio less than 0.4 (Hsu *et al.*, 1993a, Contarin *et al.*, 2005). The combined effect of the lean mixtures and low temperature gradients lead to low emissions of NO<sub>x</sub> and CO (Bingue *et al.*, 1998).

Because of these advantages, in recent years many of the researchers focus on development of porous media burner technology either experimentally or theoretically. Zhou and Pereira (1997) have performed a one-dimensional numerical simulation of methane-air flame in porous media using a multi-step reaction mechanism. They have shown that NO and CO emission is decreased significantly within porous media combustion.

A two-dimensional numerical simulation has been performed by Malico and Pereira (1999) with a single-step reaction. They have used a multi-step chemistry with 26 species and 77 reactions to analyzing pollutant formation (Malico *et al.*, 2000).

To achieve to better result in numerical simulations, it is necessary to use experimental data for porous media properties. Howell *et al.* (1995) have summarized some experimental properties such as thermal conductivity, extinction coefficient, convective heat transfer coefficient and permeability for various porous materials. Pan *et al.* (2000) have used a method combining experimental data and numerical analysis to obtain the effective heat conductivity for some ceramics. Brenner *et al.* (2000) have reported the laminar and turbulent permeability tensor, effective heat conductivity and emissivity of the porous medium as a function of temperature for Alumina fiber and Sic lamellae structure.

Some researchers have studied the effects of various porous media parameters on the combustion characteristics. Hsu *et al.* (1993) have shown the strong effect of convective heat transfer coefficient and radiative properties on the prediction of the gas and solid phase temperature field. Malico and Pereira (2001) have performed a two-dimensional numerical study on porous media combustion using the 56 approximation for solving the radiative transfer equation.

They concluded that temperature distribution is strongly dependent on radiative properties especially scattering phase function, and in the absence of radiation, the results are not in good agreement with experimental data.

Using of multi-step reaction mechanisms in numerical combustion studies leads to better prediction of combustion characteristics as well as combustion in porous media. Chen *et al.* (1987) have used a multi-step chemistry and achieved temperatures higher than adiabatic temperatures in porous media. They have shown that flame thickness in combustion zone is thicker in the case of multi-step chemistry rather than single-step reaction. Hsu and Matthews (1993) have reached the better predictions for NO, CO and CO<sub>2</sub> by adding 3 more reactions of Zeldovich NO<sub>x</sub> mechanisms. Zhou and Perreira (1998) have compared four reaction mechanisms (detailed mechanism with 277 reaction, Skeletal mechanism with 77 reactions, 4-step reduced mechanism and a single-step global mechanism) in prediction of temperature distribution and Species concentrations.

In the present study, combustion in two-dimensional porous media is numerically simulated using a multi-step mechanism and considering radiation effects of solid phase. A second order finite volume scheme is applied to discretize the conservation equations. To overcome the stiffness of system of algebraic equations, an operating splitting technique is used in which the transport and the chemical source terms are separately modeled. The method of Discrete Ordinates (DO) is used to solve the Radiative Transfer Equation (RTE). Effects of convective heat transfer coefficient and reaction mechanism are studied by comparing the numerical results with experimental data in the case of two-dimensional rectangular geometry.

## 2. Physical model

A rectangular porous burner (Fig.(1)) is used to perform numerical simulation. Some experimental and numerical information about this burner have been reported by Brenner *et al.* (2000). The burner consists of a preheat zone (zone A, 18 ppm ZrO<sub>2</sub>), a combustion zone (zone C1, 8 ppm ZrO<sub>2</sub> and zone C2, Al<sub>2</sub>O<sub>3</sub> fiber), and a heat exchanger zone to remove heat of combustion.

Physical properties of these regions such as laminar and turbulent permeability tensors and temperature dependent profile of emissivity are those reported by Brenner *et al.* (2000), but the effective heat conductivity of the porous media which includes both conductive and radiative effects of porous matrix is not used here, because in the present study two distinct energy equations are solved for the gas and solid phases and the effect of solid radiation is considered by solution of the radiative transfer equation. Also a base value of  $H_0 = 10^7 \frac{W}{m^3 \cdot K}$  is chosen for volumetric convective heat transfer coefficient.

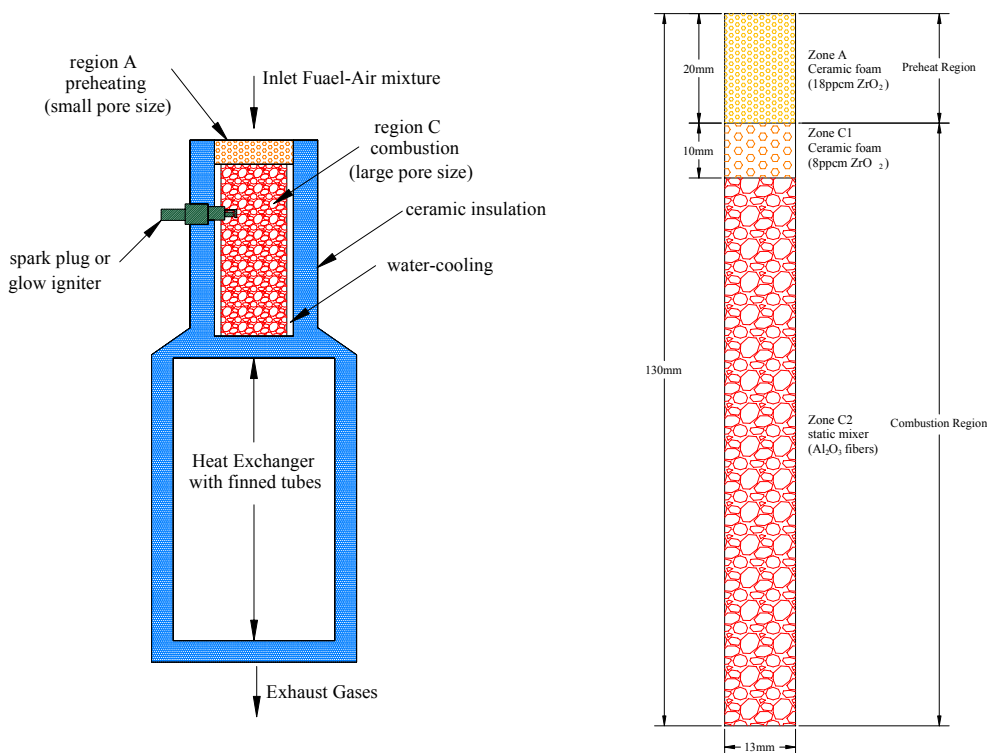


Figure 1. Porous burner geometry.

### 3. Governing Equations

#### 3.1. Conservation Equations

In the porous medium solid and fluid phases are present. The flow is influenced by the solid matrix since it occupies space and extracts energy from the reaction zone. It is assumed that the solid is chemically inert. A common method to model the porous medium is to consider it as volume averaged. There are two methods for representation of the governing equations including superficial and physical velocity formulation. The superficial velocity is related to physical velocity via:

$$\mathbf{v}_s = \phi \mathbf{v} \quad (1)$$

where  $\mathbf{v}_s$  and  $\mathbf{v}$  are superficial and physical velocity respectively, and  $\phi$  is the porosity of the media. For more accurate simulation of porous media flows, it is necessary to solve the true or physical velocity formulation. Using the physical velocity formulation, the steady state governing equation for an isotropic porous media has the following form:

##### Continuity equation:

$$\nabla \cdot (\phi \rho_f \mathbf{v}) = 0 \quad (2)$$

##### Momentum equation:

$$\nabla \cdot (\phi \rho_f \mathbf{v} \mathbf{v}) = -\phi \nabla P + \nabla \cdot (\phi \mu_f \nabla \mathbf{v}) - (\nabla P)_p \quad (3)$$

$$(\nabla P)_p = \frac{\mu_s}{k_1} \mathbf{v}_s + \frac{\mu_s}{k_2} |\mathbf{v}_s| \mathbf{v}_s \quad (4)$$

##### Gas phase energy equation:

$$\nabla \cdot (\phi \rho_f \mathbf{v} c_p T_f) = \nabla \cdot (\phi \lambda_f \nabla T_f) + \phi \sum_{k=1}^{N_s} \dot{\omega}_k h_k W_k + H (T_s - T_f) \quad (5)$$

##### Solid phase energy equation:

$$-\nabla \cdot ((1-\phi) \lambda_s \nabla T_s) = -H (T_s - T_f) - \nabla \cdot \mathbf{q}_r \quad (6)$$

##### Species conservation equation:

$$\nabla \cdot (\phi \rho_f \mathbf{v} Y_k) = \nabla \cdot (\phi \rho_f D_{km} \nabla Y_k) + \phi \dot{\omega}_k W_k, \quad k \in [1, N_s] \quad (7)$$

##### Equation of State:

$$\rho = \frac{PW_{mix}}{RT} \quad (8)$$

Equation (4) is the Forchheimer equation, which is more accurate for porous media used here, than Darcy's law. In this equation  $k_1$  and  $k_2$  are the permeability tensors for laminar and turbulent flow respectively.

The mixture dynamic viscosity,  $\mu$ , fluid heat conductivity,  $\lambda_f$ , heat capacity,  $c_p$ , heat of formation of each species,  $h_k$  and mass diffusion coefficient of each species in the mixture,  $D_{km}$  and other transport and thermodynamic data are calculated by subroutine TRANFIT (kee *et al.* (1996a)) and thermodynamic database of CHEMKINII (kee *et al.* (1996b)).

#### 3.2. Radiative Transfer Equation

The effect of solid phase radiation is taken into consideration in Eq. (6) as the divergence of the heat flux,  $(-\nabla \cdot \mathbf{q}_r)$ . For a gray medium, it can be denoted by:

$$-\nabla \cdot \mathbf{q}_r = a(r) \left[ \int_{4\pi} I(r, \Omega) d\Omega - 4\pi I_b \right] \quad (9)$$

Where  $a$  is the absorption coefficient,  $I(r, \Omega)$  the directional intensity,  $\Omega$  the direction of radiation and  $I_b$  the blackbody intensity. To find  $I(r, \Omega)$ , the RTE is solved for a gray medium:

$$(\Omega \cdot \nabla) I(r, \Omega) = a(r) I_b - (a(r) + \sigma(r)) I(r, \Omega) + \frac{\sigma(r)}{4\pi} \int_{4\pi} I(r, \Omega') \Phi(\Omega' \rightarrow \Omega) d\Omega' \quad (10)$$

where  $\sigma$  is the scattering coefficient and  $\Phi(\Omega' \rightarrow \Omega)$  is the scattering phase function. For the two-dimensional Cartesian geometry, the RTE can be expressed for each individual ordinate direction  $m$ , as:

$$\mu_m \frac{\partial(I_m)}{\partial x} + \zeta_m \frac{\partial I_m}{\partial y} - \frac{\partial(\eta_m I_m)}{\partial \psi} = -\beta I_m + a I_b + \frac{\sigma}{4\pi} \sum_{m'} w_{m'} \Phi_{m' m} I_{m'} \quad (11)$$

where  $\beta$  is the extinction coefficient,  $m$  and  $m'$  denote outgoing and incoming directions.  $\mu_m$ ,  $\zeta_m$  and  $\eta_m$  are the direction cosines of a discrete direction and  $\psi$  is the angle of revolution around x-axis. In this way Eq. (9) is written as follows:

$$\nabla \cdot \mathbf{q}_r = -a(r) \left[ 4\pi \sum_{m=1}^M I_m - 4\pi I_b \right] \quad (12)$$

Where  $M$  is the total number of ordinate directions and is related to the order of approximation  $N$ , through relationship  $M = N(N+2)/2$ . For the present work, the  $S_6$  method ( $N = 6$ ) is adapted.

#### 4. Reaction Mechanism

A reduced mechanism consisting of 15 reactions and 19 species is used (Barlow et al., 2001). These reactions with the corresponding global rates are presented in Appendix 1. The global rate for each reaction is combined of forward and backward Arrhenius rates of its elementary reactions.

#### 5. Numerical Method

The governing equations are discretized in a non-uniform structural mesh by a finite volume method. Grid independency is checked for some mesh points and finally a non-uniform mesh  $130 \times 26$  is selected where typical distances between grid points lay between 0.2 and 1 mm. Diffusive fluxes were discretized using a central difference scheme and convective fluxes are evaluated using the differed correction scheme. Pressure and the velocity are coupled by the SIMPLE algorithm of Patankar (1983).

By using a multi-step reaction mechanism, the resulting system of algebraic equations is stiff and conventional iterative methods like TDMA lead to divergence. Hence an operating splitting technique is applied to the following algorithm:

1. The velocity and pressure correction equations are solved.
2. Transient convection and diffusion of the species and of the gas energy are calculated.

$$\frac{\partial \rho Y_k}{\partial t} + \nabla \cdot (\rho \mathbf{v} Y_k) = \nabla \cdot (\rho D_{AB} \nabla Y_k) \quad (13)$$

$$\frac{\partial \rho c_p T_f}{\partial t} + \nabla \cdot (\phi \rho_f \mathbf{v} c_p T_f) = \nabla \cdot (\phi \lambda_f \nabla T_f) + H(T_s - T_f) \quad (14)$$

3. Then, the chemical reactions are dealt with by solving simultaneously the following set of equations for each control volume:

$$\frac{\partial \rho Y_k}{\partial t} = \omega_k W_k \quad (15)$$

$$\frac{\partial (\rho c_p T_f)}{\partial t} = - \sum_{k=1}^{N_{sp}} \omega_k h_k W_k \quad (16)$$

The integration time step corresponds to the minimum residence time of the gas in all the control volumes. The characteristic time scales of the chemical reactions are much smaller than the convective and diffusive transport ones.

The above equations are solved using the VODE code. (Brown *et al.*, 1989)

4. The updated mass fractions and temperatures  $[Y_i]^{new}$  and  $[T_f]^{new}$  are calculated by:

$$\begin{aligned} [Y_i]^{new} &= [Y_i]^{old} + [\Delta Y_i]^{transport} + [\Delta Y_i]^{source} \\ [T_f]^{new} &= [T_f]^{old} + [\Delta T_f]^{transport} + [\Delta T_f]^{source} \end{aligned} \quad (17)$$

## 6. Results

Figure (2) shows the temperature contours for two different equivalence ratios of 1.0 and 0.4. Figure (3) shows the species mass fraction contours. Numerical results for maximum axial temperatures are compared with experimental data of Brenner *et al.*, (2000) in Fig. (4), for the thermal powers of 2kW and 10kW. In spite of free flames in which the peak flame temperature is limited to the adiabatic flame temperature, in porous burners, peak flame temperature increases by the thermal power and may be higher than the adiabatic flame temperature. This peak flame temperature is over predicted if a single-step reaction mechanism is used. The effect of reaction mechanism on the temperature distribution and species concentration is shown in Figs. (5) and (6). The preheat zone is nearly chemically inert and independent of reaction mechanism. In addition, the multi-step mechanism considered here does not include the low temperature reactions. Global single-step reaction dictates complete combustion on the time scale of fuel disappearance, whereas multi-step mechanism stretches out the energy release process and allows for CO in the products and therefore less energy release.

The effect of volumetric heat transfer coefficient is illustrated in Fig. (7). The results are generated for an equivalence ratio of 1 and thermal power of 10kW.  $H$  is the product of convective heat transfer coefficient and the number of cells per unit length of porous matrix. The baseline value,  $H = 10^7 \frac{W}{m^3.K}$ , was chosen. As shown in the Fig. (9), in the post flame zone, the gas temperature is higher than that of the solid because the energy is released by the gas reactions and then transferred to the solid by convection. In the preflame zone, the solid temperature is higher than that of the gas because the solid is heated by radiation and then in turn convectively heats the gas. As  $H$  increases, the temperature of the solid and the gas approach each other.

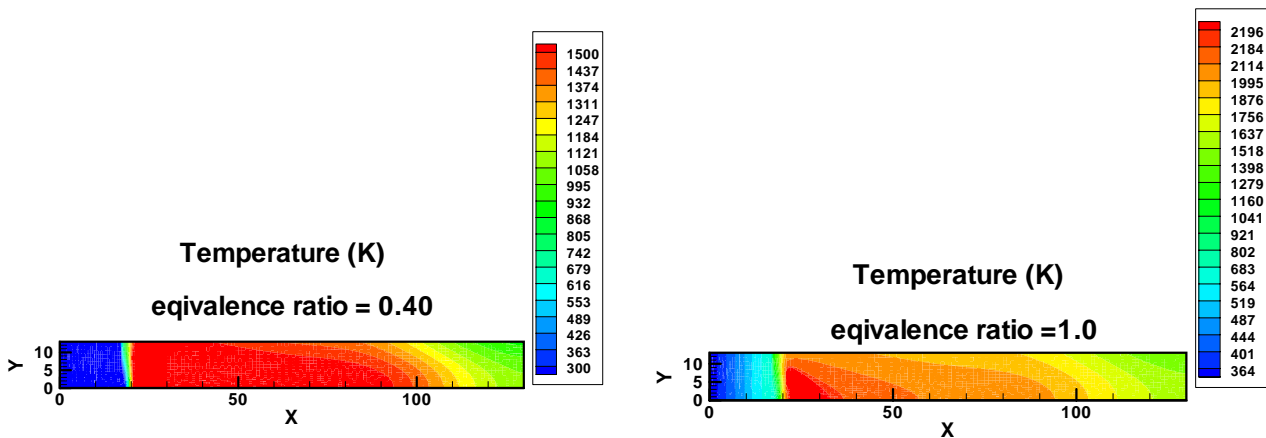


Figure 2: Ttemperature field for 10kW with two equivalence ratio of 0.4 and 1.0

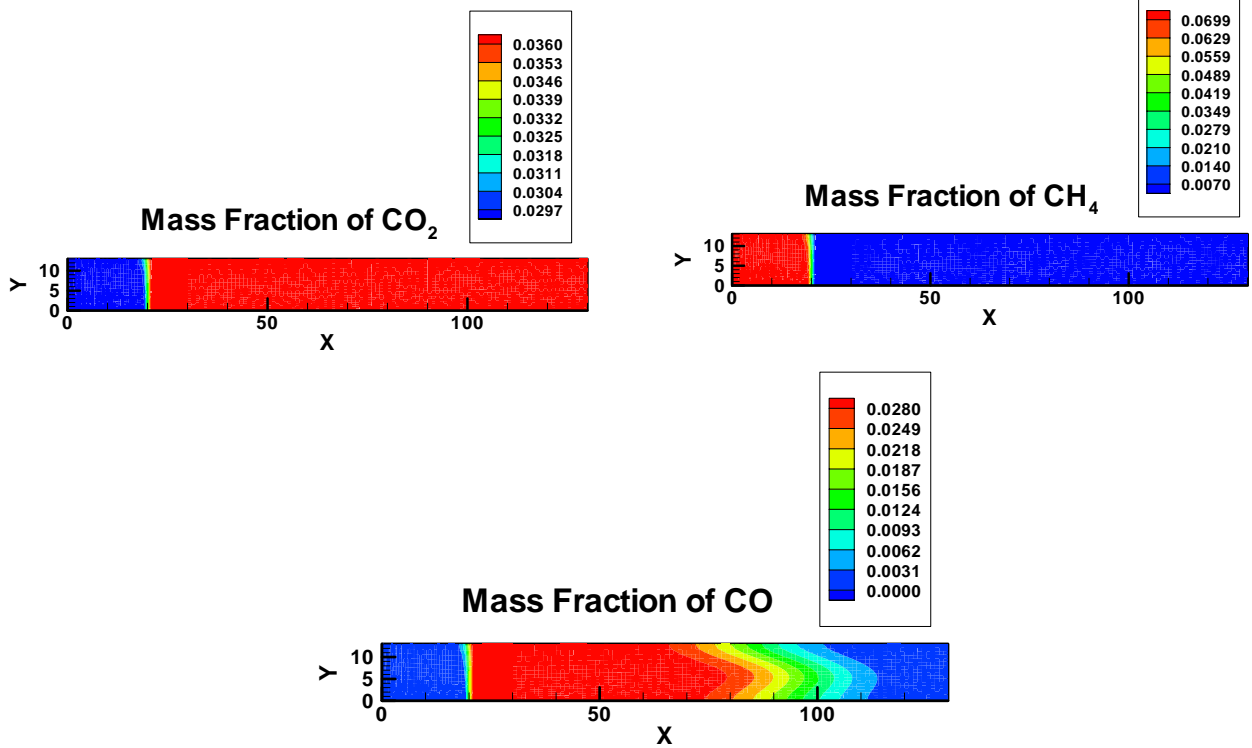


Figure 3: Contours of mass fractions of CH<sub>4</sub>, CO<sub>2</sub> and CO for 10kW and equivalence ratio of 1.

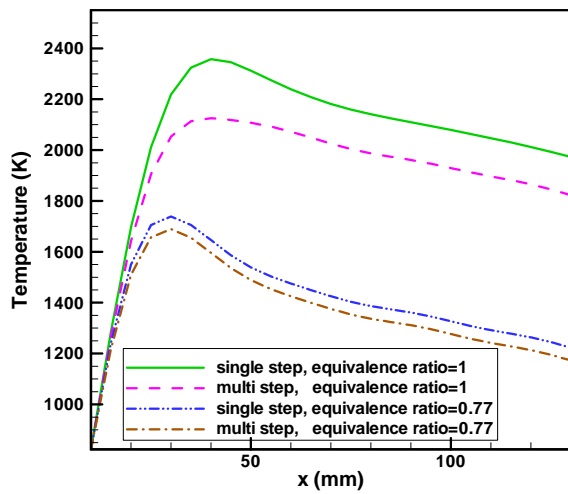


Figure 5: Effect of reaction mechanism on axial temperature for 2kW

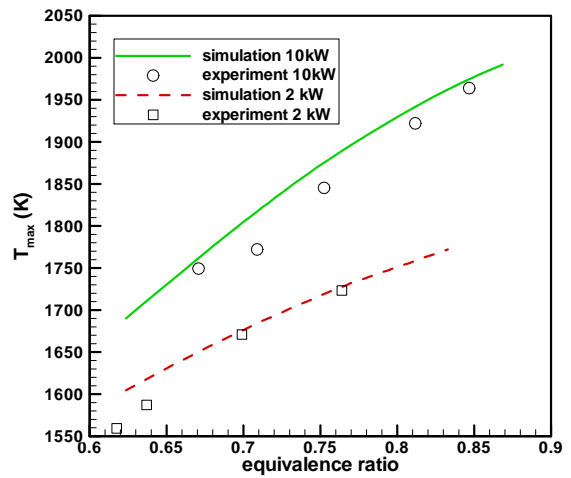


Figure 4: Maximum temperature for 2kW and 10kW

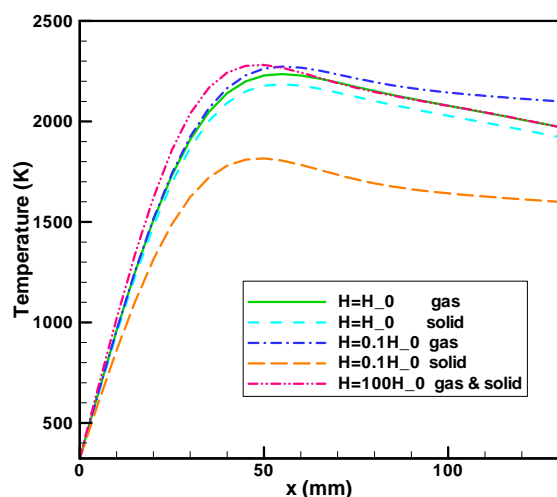


Figure 7: Effect of volumetric heat transfer coefficient on axial temperature for power of 10kW

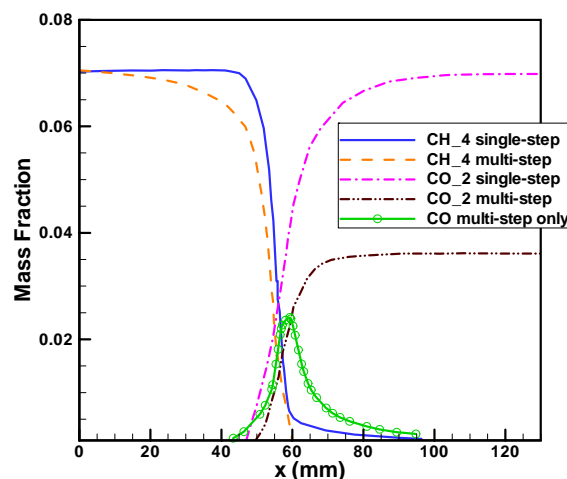


Figure 6: Effect of reaction mechanism on species mass fractions for power of 2kW

## 7. Conclusion

A two-dimensional numerical study of premixed combustion within porous inert media has been conducted. A multi-step reaction mechanism is used and radiation of the solid phase is taken into consideration using  $S_6$  discrete ordinate approximation. The effect of reaction mechanism and the volumetric heat transfer coefficient has been studied.

Due to the internal heat feedback mechanism, the porous media allows attainment of peak flame temperature that are higher than the adiabatic flame temperature. This effect is not as strong when using multi-step mechanism as is predicted by single-step mechanism. Also using of multi-step mechanism leads to improvement of the results comparing with experimental data.

## 8. References

- Babkin, V. S., 1993, "Filtration Combustion of Gases, Present and Prospects", *Pure Appl. Chem.*, Vol.65, pp. 335-344.
- Barlow, R. S., Karpetis, A. N., and Frank, J. H., 2001, "Scalar Profiles and NO Formation in Laminar Opposed-Flow Partially Premixed Methane/Air Flames", *Combust. Flame*, Vol. 127, pp. 2102-2118.
- Bingue, J. P., Saveliev, A. V., Fridman, A. A., and Kennedy, L. A., 1998, "Superadiabatic Combustion of Methane Air Mixtures Under Filtration in Packed Bed", *Combust. Flame*, Vol. 100, pp. 221-231.
- Brenner, G., Pikenacker, K., Pikenacker, O., Trimis, D., Wawrzinek, K. and Weber, T., 2000, "Numerical and Experimental Investigation of Matrix-Stabilized Methane/Air Combustion in Porous Media", *Combust. Flame*, Vol. 123, pp. 201-213.
- Brown, P. N., Byrne, G. D., and Hindmarsh, A. C., 1989, "VODE: A variable coefficient ODE solver", *SIAM J. Sci. Stat. Comput.* 10: 1038.
- Chen, Y.K., Mattews, R.D. and Howell, J.R., 1987, "The effect of Radiation on the Structure of a Premixed Flame within a highly Porous Inert Medium", *ASME HTD*, 81: 35-42.
- Contarin, F., Barcellos, W. M., Saveliev, A. V., and Kennedy, L. A., 2005, "Energy Extraction From a Porous Media Reciprocal Flow Burner With Embedded Heat Exchangers", *ASME J. Heat Transfer*, Vol. 127, pp. 123-129.
- Howell, J.R., Hall, M.J. and Ellzey, J.L., 1995, "Combustion within Porous Inert Medium", *ASME HTD, Heat Transfer in Porous Media and Two-Phase Flow*, 302: 1-21.
- Hsu, P.F., Howell, J.R., and Mettews, R.D., (1993a), "A Numerical Investigation of Premixed Combustion Within Porous Inert Media", *ASME J. of Heat Transfer*, 115: 744-750
- Hsu, P.F. and Mettews, R.D., (1993b), "The Necessity of Using detailed Kinetics in Models for Premixed Combustion Within Porous Media", *Combust. Flame*, 93: 457-466
- Kee, R. J., Dixon-Lewis, G., Warnatz, J., Coltrin, M. E. and Miler, J. A. (1996a). "A Fortran computer code package for the evaluation of gas phase multicomponent transport properties", Sandia National Lab. Report SAND86-8246.
- Kee, R. J., Miller, J. A. and Jell'erson. T. H. (1996b). "CHEMKIN: A general purpose problem independent, transportable, Fortran, chemical kinetic program package", Sandia National Lab. Report SAN80-8003.
- Malico, I. And Pereira, J.C.F, 1999, "Numerical Prediction of Porous Burners with Integrated Heat Exchanger for Household Applications", *J. Porous Media*, 2: 153-162.
- Malico, I. And Pereira, J.C.F., 2001, "Numerical Study on the Influence of Radiative Properties in Porous Media Combustion", *ASME Journal of Heat Transfer*, 123, 951-957.

- Pan, H.L., Pickenäcker, O., Pickenäcker, K., Trimis, D., and Weber, T., 2000, "Experimental Determination of Effective Heat Conductivities of Highly Porous Media", 5th European Conference on Industrial Furnaces and Boilers, Porto, 11-14.
- Patankar, S. V., 1983, "Numerical Heat transfer and Fluid Flow", McGraw Hill.
- Zhou, X.Y. and Pereira, J.C.F., 1997, "Numerical Study of Combustion and Pollutants Formation in Inert Nonhomogeneous porous Media", Combust. Sci. and Tech., 130: 335-364.
- Zhou, X.Y. and Pereira, J.C.F., 1998, "Comparision of Four Combustion Models for Simulating the Premixed Combustion in Inert Porous Media", Fire and Materials, 22: 187-197.

## Appendix 1 Reaction Mechanism

Reduced Kinetic Mechanism (Barlow et. al [14])

No.	Reaction	GLOBAL RATES FOR REDUCED MECHANISM (1/cm <sup>3</sup> .sec)
1	$H + \frac{1}{2} O_2 \leftrightarrow OH$	3.7229E-10
2	$H_2 + \frac{1}{2} O_2 \leftrightarrow H + OH$	-4.1280E-11
3	$HO_2 \leftrightarrow \frac{1}{2} O_2 + OH$	5.6583E-10
4	$\frac{1}{2} O_2 + H_2O_2 \leftrightarrow OH + HO_2$	2.0553E-13
5	$\frac{1}{2} O_2 + \frac{1}{2} C_2H_2 \leftrightarrow H + CO$	-1.4143E-11
6	$CH_3 + CO + C_2H_4 \leftrightarrow \frac{1}{2} O_2 + CH_4 + 1.50 C_2H_2$	-1.4083E-12
7	$\frac{1}{2} O_2 + 2CH_3 \leftrightarrow H_2 + CH_4 + CO$	2.6626E-11
8	$\frac{1}{2} O_2 + CH_3 \leftrightarrow H + CH_2O$	3.2685E-12
9	$\frac{1}{2} O_2 + CH_4 \leftrightarrow OH + CH_3$	2.7449E-11
10	$\frac{1}{2} O_2 + CO \leftrightarrow CO_2$	-8.6956E-14
11	$\frac{1}{2} O_2 + C_2H_6 \leftrightarrow CH_4 + CH_2O$	1.1656E-12
12	$H + OH \leftrightarrow H_2O$	9.1663E-11
13	$H + CH_4 + NO + HCN \leftrightarrow \frac{1}{2} O_2 + 2CH_3 + N_2$	1.1917E-12
14	$H + \frac{1}{2} O_2 + CH_4 + HCN \leftrightarrow 2CH_3 + NO$	-1.5580E-12
15	$\frac{1}{2} O_2 + CH_4 + NH_3 + HCN \leftrightarrow H_2O + 2CH_3 + N_2$	1.0105E-13